

1 **Testing the applicability of optically stimulated luminescence dating to Ocean Drilling**  
2 **Program cores.**

3

4 S.J. Armitage\* and R.C. Pinder†

5

6 Centre for Quaternary Research, Department of Geography, Royal Holloway, University of  
7 London, Egham, Surrey, TW20 0EX.

8

9 **Abstract**

10 Chronologies for marine sediments are usually constructed by tuning marine proxies for global ice  
11 volume ( $\delta^{18}\text{O}$ ) to the well understood variations in the Earth's orbit, by the identification of event  
12 horizons and/or by radiocarbon dating. However, these techniques are not universally applicable.  
13 Optically stimulated luminescence dating (OSL) is potentially widely applicable to marine cores  
14 and may offer significant advantages over more conventional chronometric techniques but  
15 methodological considerations regarding the application of the techniques have yet to be  
16 systematically explored. Using material from core Ocean Drilling Program (ODP) core 658B, we  
17 assess the applicability of OSL dating to deep ocean sediments. For this core, equivalent dose does  
18 not change with depth below the split core face beyond the upper 1 mm, indicating that retrieval and  
19 prolonged storage of ODP material does not compromise the OSL signal. However equivalent dose  
20 decreases with increasing particle size, reaching a plateau at ~30-40  $\mu\text{m}$ . These data suggest that  
21 ocean floor sediment reworking causes the deposition of old material at the sediment-water  
22 interface, potentially resulting in OSL age overestimates. This observation strongly suggests that  
23 seafloor reworking processes should be considered both when selecting target cores and when  
24 interpreting results. Nonetheless, we observe a good general agreement between OSL ages and

---

\* e-mail: simon.armitage@rhul.ac.uk

† Present address: Geography & Earth Sciences, Aberystwyth University, Llandinam Building, Penglais Campus, Aberystwyth, SY23 3DB, Wales, UK.

25 independent age estimates for a suite of sediments from the Marine Isotope Stage 6-5e transition,  
26 suggesting that the application of luminescence dating techniques to deep-sea sediments merits  
27 further investigation.

28

29 *Keywords:* Optically stimulated luminescence; Geochronology; Marine sediments; North Africa.

30

## 31 **1. Introduction**

32 Marine sediments are widely exploited archives of palaeoenvironmental information. Chronologies  
33 for marine sediments are usually constructed by tuning marine proxies for global ice volume ( $\delta^{18}\text{O}$ )  
34 to the well understood variations in the Earth's orbit (Lisiecki and Raymo, 2005), by the identification  
35 of event horizons such as tephras (e.g. Matthews et al., 2015) and geomagnetic excursions (e.g.  
36 Collins et al., 2012) and/or by radiocarbon dating. While tremendously powerful, these techniques  
37 are not universally applicable. Dating marine sediments using radiocarbon methods or the  $\delta^{18}\text{O}$  signal  
38 is difficult for sites below the carbonate compensation depth (e.g. much of the Southern Ocean), and  
39 radiocarbon dating is not applicable beyond ~50-60 ka even where carbonate is preserved. Correlation  
40 of the  $\delta^{18}\text{O}$  record from a particular core to a "stacked" record (e.g. Lisiecki and Raymo, 2005) is  
41 often complicated by site specific factors such as: 1) hiatuses in the depositional record due to bottom  
42 current reworking; 2) smoothing of the  $\delta^{18}\text{O}$  signal by bioturbation, such that only the most  
43 pronounced events are discernible and 3) misidentification of events in complex isotopic stages such  
44 marine isotope stage (MIS) 5. Event horizons such as tephras are invaluable in integrating marine and  
45 terrestrial records, but are only useful where their occurrence is frequent in the period of interest. In  
46 addition, accurate identification of both tephra horizons and geomagnetic excursions in marine cores  
47 frequently requires an initial lower-precision age model e.g. where a single source emits multiple  
48 geochemically similar tephras, such as the Campi Flegrei between c. 17-14 ka BP (Matthews et al.,  
49 2015). These limitations have rendered some timeframes and regions difficult to date. For example,  
50 in the carbonate free regions of the Arctic Ocean, competing chronostratigraphic interpretations yield

51 sedimentation rates which differ by an order of magnitude (Berger, 2006). Consequently, several  
52 authors (e.g. Armitage, 2015; Berger, 2006; Jakobsson et al., 2003; Stokes et al., 2003) have  
53 advocated the use of optically stimulated luminescence (OSL) as an additional method to provide age  
54 information for deep-sea sediments.

55  
56 OSL is a radiometric dating technique which determines the time elapsed since a mineral grain  
57 (usually quartz or feldspar) was last exposed to sunlight (i.e. burial period) and has gained wide  
58 acceptance as a tool for developing terrestrial chronologies (Olley et al., 2004). An OSL age is  
59 calculated using Equation 1:

$$60$$
$$61 \text{ Age (ka)} = \text{Equivalent dose (Gy)} / \text{Dose rate (Gy/ka)} \quad (\text{Eq. 1})$$

62  
63 where the equivalent dose ( $D_e$ ) is the laboratory estimate of the cumulative exposure of a sample to  
64 ionising radiation since deposition, and the dose rate is the rate of exposure to ionising radiation. In  
65 principle, luminescence methods can date any marine sediment containing quartz (to ~200 ka) or  
66 feldspar (to ~500 ka), provided that these minerals were subaerially exposed immediately prior to  
67 deposition. However, a number of potential impediments to the routine application of OSL dating to  
68 deep-sea sediments, relating to determination of both the equivalent dose and the dose rate, have been  
69 identified. Determination of a chronologically useful equivalent dose may be hampered by: 1) the  
70 incorporation of material which was not exposed to sufficient sunlight prior to deposition to  
71 completely reset the OSL signal (Berger, 2006); 2) depletion of the OSL signal due to light exposure  
72 during core retrieval and storage, and 3) reworking of older material into sediments during deposition,  
73 leading to an overestimation of the depositional age (Armitage, 2015; Berger, 2006). Accurate  
74 determination of the dose rate for deep-sea sediments is complicated by disequilibrium in the uranium  
75 decay series due to incorporation of excess long-lived insoluble isotopes ( $^{230}\text{Th}$  in the  $^{238}\text{U}$  series and  
76  $^{231}\text{Pa}$  in the  $^{235}\text{U}$  series) into seafloor sediments (Stokes et al., 2003; Wintle and Huntley, 1979) and

77 authigenic uranium uptake at the sediment-water interface under reducing conditions (Armitage,  
78 2015).

79

80 In this study we use sediment from Ocean Drilling Program (ODP) core 658B (Ruddiman et al., 1988)  
81 to test the applicability of optically stimulated luminescence dating to marine sediments. Specifically  
82 we aim to: 1) assess directly the depletion of the OSL signal due to light exposure during core retrieval  
83 and storage; 2) test the hypothesis (Armitage, 2015) that coarser quartz grains are less prone to  
84 seafloor reworking and hence are the preferred dosimeter for OSL dating of deep-sea sediments, and  
85 3) test the applicability of OSL to sediments beyond the range of  $^{14}\text{C}$  by dating known-age material  
86 from marine isotope stage MIS 6-5e.

87

## 88 **2 Materials and methods**

89 Core 658B was recovered in 1986 from a water depth of 2,263 m off Cap Blanc, Mauritania  
90 (20°45'N, 18°35'W) during ODP Leg 108 (Ruddiman et al., 1988). Trade winds cause strong  
91 upwelling over the site, leading to high surface productivity and high biogenic particle fluxes to the  
92 seafloor. Biogenic carbonate comprises 40-60% by mass of the sediment, and until recently the  
93 remainder was thought to consist of terrigenous dust (deMenocal et al., 2000) due to the site's  
94 location beneath the axis of the summer African dust plume (Figure 1). However, recent analysis of  
95 orbital radar satellite imagery has been used to propose that during the late-glacial to Holocene  
96 African Humid Period (~11.5-5 ka, Armitage et al., 2015; deMenocal et al., 2000; McGee et al.,  
97 2013) a major river within the Tamanrasset palaeowatershed delivered large amounts of fluvial  
98 sediment to this site (Skonieczny et al., 2015). Irrespective of the transport pathway followed by  
99 terrigenous sediments in ODP Core 658B, Armitage (2015) was able to measure OSL ages which  
100 were consistent with independent chronological information over the timeframe ~10-50 ka,  
101 suggesting that the OSL signal in this material was completely reset by subaerial exposure  
102 immediately prior to deposition.

103

104 Core 658B is an ideal target for testing OSL dating in the marine realm since: 1) It has a high  
105 accumulation rate (c.18 cm/ka, deMenocal et al., 2000); 2) The high terrigenous sediment flux  
106 provides a substantial well-bleached quartz component; 3) The terrigenous sediments have a  
107 sufficiently wide grain-size range to test the hypothesis that coarse grains are less prone to seafloor  
108 reworking; 4) The excess  $^{230}\text{Th}$  ( $^{230}\text{Th}_{\text{xs}}$ ) record for core Core 658C (Adkins et al., 2006) may be  
109 used to calculate excess activity in Core 658B and 5) Core 658B was 16 years old when sampled so  
110 the deleterious effects (if any) of light exposure during storage should be pronounced.

111

## 112 **2.1 Equivalent dose determination**

113 Samples were collected in July 2002 from a 66 mm diameter split core at the ODP East Coast  
114 Repository, Lamont-Doherty Earth Observatory, USA. Paired samples were taken every ~25 cm  
115 through the uppermost 11 m of the core by inserting short sections of 20 mm diameter opaque  
116 tubing. This approach yielded two ~7 cm<sup>3</sup> sub-samples per level. Samples were processed under  
117 subdued orange light at the Royal Holloway luminescence laboratory. In all cases the outer (closest  
118 to the core barrel) ~8 mm was discarded to avoid core barrel smearing (Figure 2). For the samples  
119 presented in Sections 4 and 5 the light exposed upper (split core face) ~8 mm was removed and  
120 used for carbonate content and dose rate analysis, while the remaining middle ~8 mm of the sample  
121 was dispersed in deionised water and sieved at 150  $\mu\text{m}$ . The  $>150 \mu\text{m}$  fraction consisted of  
122 foraminiferal tests, and  $<150 \mu\text{m}$  fraction was used for equivalent dose measurements. For the  
123 samples presented in Section 3, the upper 5 mm of sediment was removed in 1 mm thick slices, and  
124 an equivalent dose was measured for material from each slice. Equivalent doses were measured on  
125 quartz isolated from samples by treating them with HCl and H<sub>2</sub>O<sub>2</sub> to remove carbonate and organic  
126 matter respectively. The resulting material was then separated into the required size fraction using  
127 Stokes settling for fractions  $\leq 20 \mu\text{m}$  and wet sieving for larger fractions, and feldspar was  
128 subsequently removed using H<sub>2</sub>SiF<sub>6</sub> followed by an HCl rinse.

129

130 All OSL measurements presented in this study were carried out using a Risø TL/OSL-DA-20  
131 automated dating system. Optical stimulation of single aliquots was carried out using a blue ( $470 \pm$   
132  $30$  nm) light emitting diode (LED) array with a power density of  $\sim 90$  mW/cm<sup>2</sup>. Infra-red (IR)  
133 stimulation was carried out using an IR (870 nm) laser diode array with a power density of  $\sim 200$   
134 mW/cm<sup>2</sup>. OSL was measured using an Electron Tubes Ltd 9235QB photomultiplier tube with 7.5  
135 mm of Hoya U-340 filter interposed between the sample and photomultiplier. Irradiation was carried  
136 out using a 40 mCi <sup>90</sup>Sr/<sup>90</sup>Y beta source, calibrated relative to the National Physical Laboratory,  
137 Teddington Hotspot 800 <sup>60</sup>Co  $\gamma$ -source (Armitage and Bailey, 2005). Equivalent doses ( $D_e$ ) were  
138 determined using the single-aliquot regenerative-dose (SAR) method (Galbraith et al., 1999; Murray  
139 and Wintle, 2000). OSL signals were measured at 125 °C and growth curves were fitted using a  
140 saturating-exponential-plus-linear function. The standard error associated with each individual  $D_e$   
141 determination was estimated by Monte Carlo simulation using Luminescence Analyst Software  
142 (Duller, 2007). Previous dose recovery experiments (Roberts et al., 1999; Wallinga et al., 2000) on  
143 quartz from ODP Core 658B found no dependence of  $D_e$  upon preheating regime for three samples  
144 with equivalent doses ranging from 23-77 Gy (Armitage, 2015). An additional dose recovery  
145 experiment was performed on sample 73B ( $D_e = 198$  Gy), which confirmed that this finding is also  
146 true for the older samples reported in Section 5. Preheating regimes of 260 °C, 10 s for PH1 (the pre-  
147 heat prior to measurement of  $L_n$  or  $L_x$ ) and 220 °C, 10 s for PH2 (the pre-heat prior to measurement  
148 of  $T_n$  or  $T_x$ ) or 200 °C, 10 s for PH1 and 160 °C, 0 s for PH2 were adopted for all subsequent  
149 measurements. When calculating  $D_e$ , aliquots were rejected where the recycling ratio (Murray and  
150 Wintle, 2000) or IR depletion ratio (Duller, 2003) differed from unity by more than two standard  
151 deviations, or where the sensitivity corrected luminescence intensity in response to a 0 Gy  
152 regeneration dose exceeded 5% of the sensitivity corrected natural luminescence intensity.

153

## 154 **2.2 Dose rate calculation**

155 The environmental dose rate for MIS 6-5e samples from core 658B was calculated using a version of  
156 the  $\text{Marine}_{\text{xs+auth}}$  model described in Armitage (2015). Briefly,  $^{238}\text{U}$  and  $^{232}\text{Th}$  and bulk K  
157 concentrations were measured using ICP-MS. Authigenic uranium ( $\text{U}_{\text{auth}}$ ) activity was calculated  
158 using the  $^{238}\text{U}/^{232}\text{Th}$  activity ratio of crustal rocks and pelagic marine sediments of  $0.8\pm 0.2$  (Anderson  
159 et al., 1989), and corrected for the effects of ingrowth of  $^{230}\text{Th}$  from  $^{234}\text{U}_{\text{auth}}$  (Section S1). Burial  
160  $^{230}\text{Th}_{\text{xs}}$  for all samples was assumed to be the mean value ( $36.6\pm 9.3$  Bq/kg) measured by Adkins et  
161 al. (2006) for Core 658C over the time period 2-18.5 ka. Initial  $^{231}\text{Pa}_{\text{xs}}$  ( $3.38\pm 0.87$  Bq/kg) was  
162 calculated using the 0.093 production activity ratio of  $^{231}\text{Pa}/^{230}\text{Th}$  (Henderson and Anderson, 2003).  
163 Time independent dose rates were calculated from detrital  $^{238}\text{U}$  (measured  $^{238}\text{U}$  minus  $\text{U}_{\text{auth}}$ ),  $\text{U}_{\text{auth}}$ ,  
164  $^{232}\text{Th}$  and K concentrations, assuming equilibrium for  $^{238}\text{U}$  and  $^{232}\text{Th}$ , and equilibrium from  $^{238}\text{U}$ - $^{234}\text{U}$   
165 for  $\text{U}_{\text{auth}}$ , using the standard conversion factors (Guérin et al., 2011). The additional time dependant  
166 dose contribution due to  $^{230}\text{Th}_{\text{xs}}$  and  $^{231}\text{Pa}_{\text{xs}}$ , and the final age calculation, were performed using the  
167 method outlined by Stokes et al. (2003). Dose rates were corrected for alpha efficiency ( $0.02\pm 0.02$ ),  
168 alpha and beta attenuation and water content (Aitken, 1985). Water contents were taken from the  
169 relevant ODP initial report (Ruddiman et al., 1988). Dose rate data and ages are presented in Tables  
170 S1 and S2. The dose rate values for individual isotopes within the uranium and thorium decay series  
171 provided in Tables 5-12 of Stokes et al. (2003) are based upon outdated dose rate conversion factors  
172 (Adamiec and Aitken, 1998). Updated values based upon the conversion factors of Guérin et al.  
173 (2011) are provided in supplementary data Tables S3-S6.

174

### 175 **3 Assessment of OSL signal depletion during core retrieval and storage**

176 For OSL dating of marine sediments to become a useful tool for the palaeoclimate community, the  
177 technique must be applicable to curated material. However, few marine cores have been retrieved or  
178 stored with the intention of preserving their luminescence signal, and consequently most have been  
179 exposed to unquantified amounts of light, possibly compromising their use for OSL dating. ODP  
180 cores are stored under cool ( $4\text{ }^{\circ}\text{C}$ ) moist conditions, preventing desiccation and shrinkage, meaning

181 that only the split core face is exposed to laboratory light. Consequently signal loss due to light  
182 exposure during storage should be greatest at the core face, and reduce to a negligible level with  
183 depth. To determine the depth below which negligible signal loss occurred during storage,  $D_e$ -depth  
184 profiles were constructed for two samples (Figure 3). The fine silt (4-11  $\mu\text{m}$ ) fraction was used for  
185 these measurements since it is sufficiently abundant to allow assessment of very small sample  
186 volumes. The  $D_e$ -depth profile for sample 6B is flat, while the profiles for sample 7B has a plateau in  
187  $D_e$  below 1 mm depth.

188

189 We interpret these data to indicate that for ODP core 658B,  $\leq 1$  mm of sediment is required to  
190 completely shield underlying material from bleaching by laboratory light. This result is consistent  
191 with similar studies which have demonstrated that the effects of brief sunlight bleaching on TL only  
192 extended  $\sim 2$  mm into a quartzite pebble (Richards, 1994), while  $< 10$  mm of sandy limestone  
193 prevented bleaching of the OSL signal during  $\sim 5,000$  years of exposure to direct Saharan sunlight  
194 (Armitage and King, 2013). Since core 658B was sampled 16 years after it was split, it is probable  
195 that similarly curated cores also preserve a useable amount of material which is suitable for OSL  
196 dating, and the technique may be applied retrospectively to a wide range of archived marine cores.

197

#### 198 **4. Equivalent dose versus grain-size**

199 The fine-silt component of marine sediment is prone to seafloor reworking by bottom-currents. Since  
200 this reworking occurs at depth and in darkness, the reworked sediment is deposited with a  
201 luminescence signal due to the cumulative radiation exposure experienced since sub-aerial exposure  
202 to sunlight. Consequently, the equivalent dose for this material does not relate solely to the time  
203 elapsed since final deposition, leading to age overestimates when luminescence dating is applied to  
204 minerals extracted from this size-fraction (Armitage, 2015; Berger, 2006, 2009, 2011). However,  
205 bottom-current reworking processes should be most important for finer grain-size fractions, owing to  
206 the strong dependence of settling velocity upon particle size. For example, 90% of grains within the

207 nepheloid (cloudy) layer in non-polar deep oceans, which results from bottom-current reworking  
208 processes, consists of grains with a diameter for 0.5-8.5  $\mu\text{m}$  (Berger, 2006). These considerations  
209 suggest that where bottom-current reworking may have occurred, deep-sea sediments should be dated  
210 using mineral grains extracted from the coarsest fraction possible. Unfortunately, the dominant  
211 minerogenic fraction of many marine sediments is fine silt sized, and few cores are physically large  
212 enough to allow the study of fractions which are not abundant. Consequently, it is important to  
213 determine the minimum grain size which is not subject to bottom-current reworking.

214

215 ODP site 658 is ideal for studying seafloor reworking since despite being located on a ridge between  
216 two major submarine canyon systems (Ruddiman et al., 1988),  $^{230}\text{Th}_{\text{xs}}$  measurements suggest that  
217 core 658C has received three time more sediment laterally than vertically over the last 20 ka (Adkins  
218 et al., 2006). This observation led Armitage (2015) to argue that the discrepancy between paired fine  
219 silt (4-11  $\mu\text{m}$ ) and coarse silt (40-63  $\mu\text{m}$ ) luminescence ages for core 658B were due to the  
220 incorporation of “old” reworked material into the former. In addition, ODP site 658’s location beneath  
221 the summer African dust plume (deMenocal et al., 2000) and offshore of a major river (Skonieczny  
222 et al., 2015) mean that it contains dateable quantities of fine and coarse silt-sized quartz.

223 Equivalent doses were measured from the 0-5, 5-10, 10-15, 15-20, 20-30, 30-40 and 40-60  $\mu\text{m}$   
224 fractions of samples 12B and 15B (Figure 4). These samples were measured due to the discrepancy  
225 between the fine and coarse silt luminescence ages reported by Armitage (2015), and due to the  
226 agreement between the latter and the independent chronology for core 658B. For each sample,  
227 equivalent doses were normalised to the  $D_e$  measured from the 40-63  $\mu\text{m}$  fraction after correction for  
228 grain size dependant variation in both instrument (Armitage and Bailey, 2005) and environmental  
229 (Durcan et al., 2015) dose rates. For both samples, the normalised  $D_e$  decreases with increasing grain  
230 size, and  $D_e$  for the 30-40  $\mu\text{m}$  grains is indistinguishable from that for 40-60  $\mu\text{m}$ . However, the  $D_e$   
231 for the finest fraction (0-5  $\mu\text{m}$ ) of 12B was nearly twice that for the coarsest fraction (40-60  $\mu\text{m}$ )  
232 whereas the discrepancy was 20% for sample 15B.

233

234 From these data we infer that at ODP site 658, reworked older material is present in size fractions as  
235 coarse as 20-30  $\mu\text{m}$ , and is not restricted to the fine silt fraction as might have been expected from  
236 the composition of the nepheloid layer. The progressive decrease in  $D_e$  with increasing grain size  
237 suggests that the proportion of reworked material present is similarly decreasing. Consequently it is  
238 possible that at sites which are subject to less lateral sediment movement than ODP 658, grain sizes  
239 finer than 20-30  $\mu\text{m}$  might produce reliable ages. The main tool for determining the presence or  
240 absence of lateral sediment movement is  $^{230}\text{Th}_{\text{xs}}$  measurements (Adkins et al., 2006). However, since  
241 this technique relies on discrepancies between the abundance of  $^{230}\text{Th}_{\text{xs}}$  in samples, and the rate of  
242  $^{230}\text{Th}_{\text{xs}}$  production in the overlying water column, it may only be used for well-dated depth intervals  
243 (Adkins et al., 2006). Consequently, an alternative method for testing for reworked sediment is  
244 required. Where a sufficiently wide range of grain sizes are present in a single sample, the absence of  
245 change in  $D_e$  with grain size provides strong circumstantial evidence for the absence of older  
246 reworked material. Nonetheless the discrepancy between the scale of grain size dependence for  
247 samples 12B and 15B suggests that the incorporation of reworked material is highly temporally  
248 variable. Consequently,  $D_e$  versus grain size measurements would need to be made on a number of  
249 samples from any given site to make a strong case that reworked sediment was absent. These  
250 conclusions do not preclude the application of luminescence dating to marine sediments, but they do  
251 strongly suggest that seafloor reworking processes should be considered both when selecting target  
252 cores and when interpreting results. However, since fine grained particles may be redeposited into  
253 deep-sea sediments by turbidity (downslope) and contour (along-slope) currents, consideration of  
254 contour current velocity alone is unlikely to be sufficient (Faugères and Mulder, 2011).

255

## 256 **5. Dating samples from MIS 6-5**

257 A number of studies have demonstrated good agreement between independent chronologies and  
258 luminescence ages from deep-sea sediments. In most cases these studies used material retrieved from

259 relatively shallow depths where  $^{230}\text{Th}_{\text{xs}}$  and  $^{231}\text{Pa}_{\text{xs}}$  is insignificant, and/or have used cores where  
260 detrital terrigenous inputs are sufficiently large to render these excess activities insignificant in the  
261 dose rate calculation. Of the studies that have accounted for  $^{230}\text{Th}_{\text{xs}}$  and  $^{231}\text{Pa}_{\text{xs}}$ , few provide  
262 convincing ages beyond the range of  $^{14}\text{C}$  (e.g. Stokes et al., 2003). However, it is essential to  
263 demonstrate the applicability of luminescence dating to these older samples if the technique is to  
264 become established as a useful chronometer for marine sediments. To provide a convincing test of  
265 luminescence dating as applied to deep-sea sediments beyond the range of  $^{14}\text{C}$ , it is necessary to  
266 identify samples with precisely and accurately known ages. Samples which meet these criteria have  
267 proved difficult to identify in terrestrial settings (e.g. Murray et al., 2008; Murray and Funder, 2003;  
268 Murray et al., 2007) but ought to be relatively easy to identify in marine settings with continuous  
269 sedimentation and a well-resolved  $\delta^{18}\text{O}$  record or (well-dated) unambiguously identifiable event  
270 horizons. For example, Stokes et al. (2003) used the Toba Ash and last appearance of *Globigerinoides*  
271 *ruber* (pink) to provide known age horizons at ~74 and ~120 ka. In the present case, an independent  
272 age was estimated for each sample by identifying MIS 5e (sample 69B) and MIS 6 (sample 77A) in  
273 our  $\delta^{18}\text{O}$  record, and assigning these samples ages of 123 and 140 ka respectively (Lisiecki and  
274 Raymo, 2005). Ages for samples between these two points were estimated assuming a constant  
275 accumulation rate. Ages were measured for eight samples, using coarse silt-sized (40-63  $\mu\text{m}$ ) quartz.  
276 Equivalent doses, dose rates and ages for these samples are presented in Tables S1 and S2. Coarse  
277 silt OSL ages are shown alongside the independent chronological data in Figure 5.

278

279 All the luminescence ages are in agreement with the independent ages estimated from the  $\delta^{18}\text{O}$  record.  
280 However, although individual pairs of luminescence and independent ages are indistinguishable,  
281 principally due to the ~6-9% uncertainty on the former, all eight luminescence ages are lower than  
282 their respective independent ages. Dose recovery experiments were performed on 10 aliquots of  
283 samples 74B and 75B, using given doses of 220 and 240 Gy respectively, and yielded mean ratios  
284 (measured/given) of  $1.04 \pm 0.02$  and  $1.02 \pm 0.02$ . These data suggest that the measurement procedure

285 adopted is appropriate for these samples. However, the mean ratio of OSL to independent ages is  
286  $0.93\pm 0.04$ . In an attempt to determine the cause of this age underestimate, the OSL data were  
287 repeatedly reanalysed. Firstly, aliquots were rejected where the recycling ratio or IR depletion ratio  
288 differed from unity by more than one standard deviation. This approach reduced the yield of  
289 acceptable aliquots from 86 to 59%, but the mean ratio of original: recalculated equivalent doses was  
290  $1.00\pm 0.01$ , suggesting that insufficiently stringent rejection criteria do not account for the observed  
291 age underestimate. Using an early-background subtraction (Cunningham and Wallinga, 2010)  
292 yielded a ratio of  $1.01\pm 0.01$  (signal and background intervals of 0-0.2 and 0.2-0.7 s as opposed to 0-  
293 0.2 and 36-40 s in the original analysis) suggesting that the initial signal is fast-component dominated.  
294 Similarly, integrating the signal from 0.1-0.3 s yielded a ratio of  $0.98\pm 0.01$ , indicating that an unstable  
295 ultrafast component is not present (Jain et al., 2008). Lastly, excluding aliquots where  $D_e$  is greater  
296 than twice the curve fitting parameter  $D_0$  when the growth curve is fitted using a single saturating  
297 exponential fit (Durcan, 2012; Wintle and Murray, 2006) yielded a ratio of original to recalculated  
298 equivalent doses of  $0.96\pm 0.02$ . This, combined with the observation that for all aliquots the  
299 sensitivity-corrected luminescence intensity continues to grow with dose beyond  $D_e$ , leads us to infer  
300 that the observed age underestimate is not caused by dose-response saturation.

301

302 The mean ratio of OSL to independent ages ( $0.93\pm 0.04$ ) is similar in magnitude to the discrepancy  
303 between OSL and “known” ages reported for several terrestrial Eemian sites (e.g. Murray and Funder,  
304 2003; Murray et al., 2007) which are approximately contemporaneous with our material. However,  
305 quartz OSL age underestimates are not universally found for Eemian and pre-Eemian sites (e.g.  
306 Murray et al., 2008), and despite considerable research it has proved difficult to identify a mechanism  
307 explaining the age underestimates which are found (e.g. Lowick and Preusser, 2011). It is possible  
308 that our ages for MIS 6-5e samples from core 658B are another example of this phenomenon. It is  
309 equally plausible that age underestimates result from the use of  $^{230}\text{Th}_{\text{xs}}$  data from the 2-18.5 ka portion  
310 of the core (Adkins et al., 2006), which may not be representative of conditions during the MIS 6-5e

311 transition. Nonetheless, the general agreement between our ages and independent age estimates  
312 indicates that luminescence dating of deep-sea sediments beyond the range of  $^{14}\text{C}$  is possible.

313

## 314 **6. Conclusions**

315 Our data from ODP core 658B suggest that a wide range of marine sediments may be suitable for  
316 OSL dating. In particular, prolonged storage in core repositories does not reduce the OSL signal,  
317 except for material less than 1 mm below the exposed surface, meaning that most archived cores  
318 should be suitable for OSL dating. However, seafloor reworking is not restricted to fine silt sized  
319 particles as had been suggested by previous authors. At Site 658, this process appears to be  
320 responsible for the redeposition of particles as large as 20-30  $\mu\text{m}$  in diameter. This finding suggests  
321 that seafloor reworking may be a primary determinant of the applicability of luminescence dating to  
322 deep ocean sediments. Nonetheless, it may frequently be possible to work on sites or particle sizes  
323 which are not subject to seafloor reworking. Lastly, our data indicate that accurate luminescence  
324 dating of deep-sea sediments beyond the range of  $^{14}\text{C}$  is possible, and suggest that this application  
325 of the technique merits further investigation.

326

## 327 **7 Acknowledgements**

328 Sample collection, calcium carbonate analysis and radioisotope and  $\delta^{18}\text{O}$  measurements were funded  
329 by NERC grant NER/T/S/2001/01236 awarded to Stephen Stokes. Calcium carbonate analysis and  
330 foraminifera picking for  $\delta^{18}\text{O}$  measurements was carried out by Chris Beer and Abigail Stone. Jenny  
331 Kynaston drew Figure 1 and Malcolm Kelsey drew Figure 2.

332

## Figure captions

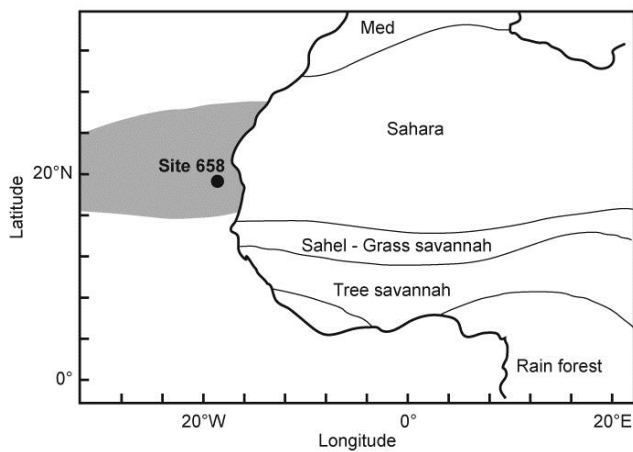


Figure 1: Location of ODP Site 658 under the summer African dust plume (grey). Redrawn from deMenocal et al. (2000).

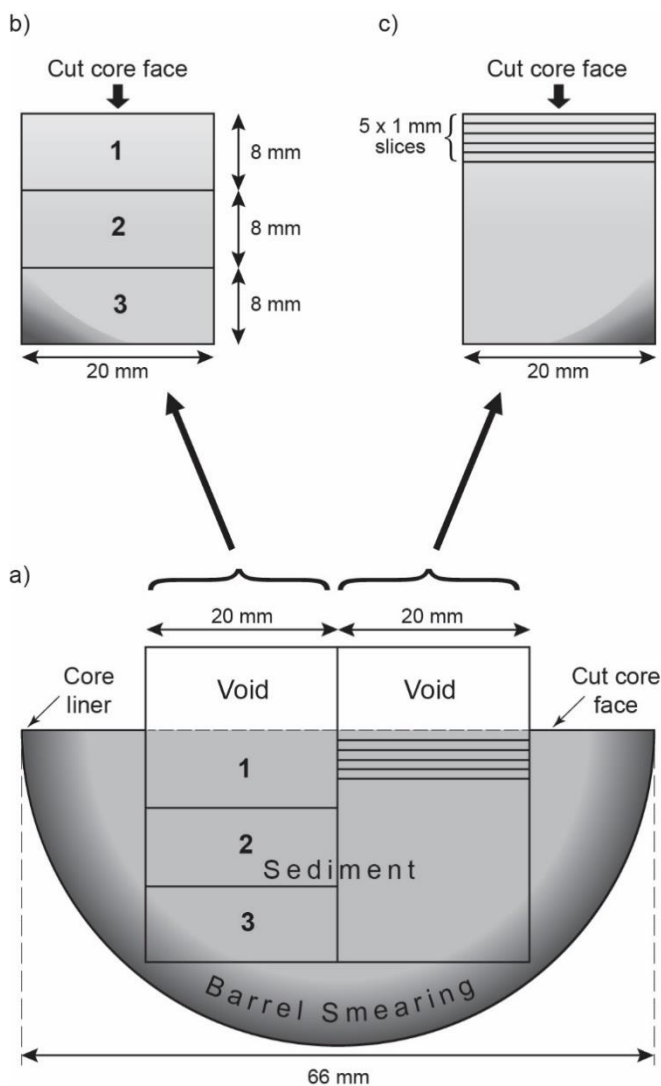


Figure 2: Sampling of ODP core 658B. a) The split core showing core dimensions, the cut core face, which is assumed to be bleached by core repository lighting, and barrel smearing i.e. sediment intruded into underlying material during coring. OSL samples were taken by pushing two 20 mm diameter opaque tubes into the cut core face. b) Typical sub-samples taken from a single OSL

sample tube. This sub-sampling scheme was followed for material presented in Sections 4 and 5. Section 1 contains the light exposed core face and was used for carbonate content and dose rate evaluation. Section 2 was used for equivalent dose determination while section 3 was discarded as containing some contamination due to barrel smearing. c) Sub-sampling scheme used to produce the  $D_e$ -depth profiles presented in Section 3.

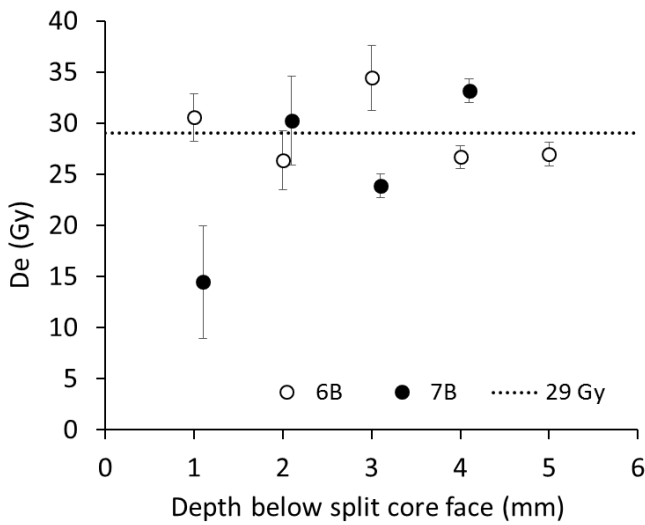


Figure 3: Equivalent dose versus depth below split core face for samples 6B and 7B. Markers are centred upon the mean  $D_e$  on the y-axis, and the deepest depth represented in the sample on the x-axis. Each point is the mean of 3-6 aliquots, and 6 aliquots were measured where sufficient material was available. Data for sample 7B are offset by 0.2 mm on the x-axis for clarity. The dashed line is at 29 Gy, the approximate  $D_e$  for the 8-16 mm depth subsample of both samples (6B =  $28.99 \pm 1.07$  Gy and 7B =  $29.08 \pm 1.07$  Gy, Armitage, 2015)

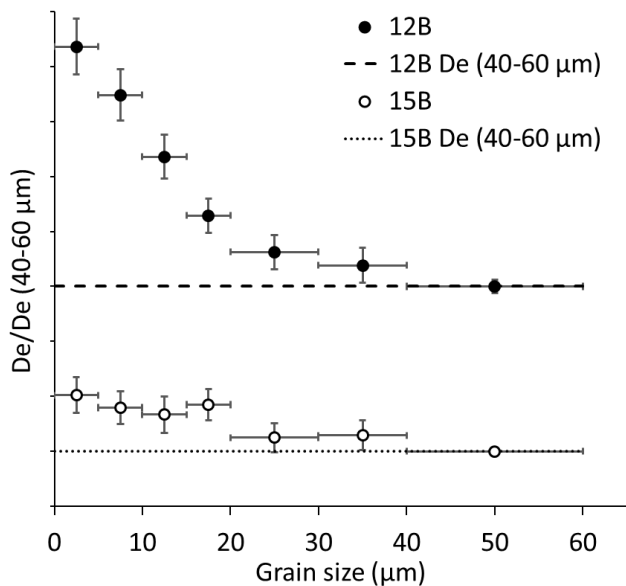


Figure 4: Equivalent dose (normalised to the equivalent dose for the 40-60  $\mu\text{m}$  fraction) versus grain size for samples 12B and 15B. Markers are centred upon the mean normalised  $D_e$  on the y-axis, and the mean grain size on the x-axis. Each point is the mean of 6-9 aliquots, and 9 aliquots were measured where sufficient material was available. Equivalent doses were corrected for the grain size dependency of instrument and environmental dose rates (Armitage and Bailey, 2005; Durcan et al., 2015) and normalised to the data for 40-60  $\mu\text{m}$ . A 3% uncertainty was assumed on each correction factor. X-axis uncertainties indicate the range of grain sizes in a fraction, while the

y-axis uncertainties were calculated via the propagation in quadrature of errors on the measured equivalent dose, instrument beta source calibration (3%), grain-size specific instrument dose rate correction factor (3%) and grain size specific environmental dose rate correction factor. Y-axis tick marks are spaced at 0.2 (20%) intervals.

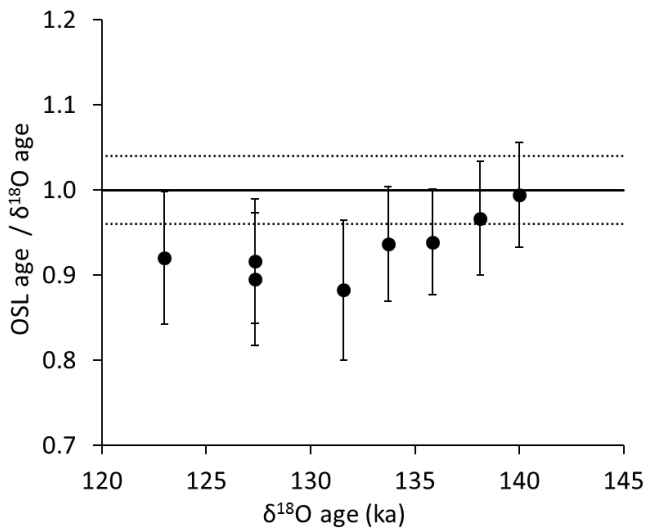


Figure 5: OSL age (normalised to the independent age determined via comparison of our  $\delta^{18}\text{O}$  record to the LR04 stack – “ $\delta^{18}\text{O}$  age”) versus independent age for coarse silt-sized quartz samples from the MIS6-5e section of core 658B. Nine aliquots were measured for each sample, and two separately prepared sub-samples of sample 71 (127 ka) were measured. The solid line represents a normalised OSL age of unity (OSL age = independent age) while the dashed lines at  $\pm 4\%$  of this value represent the claimed uncertainty on ages attributed to isotopic events in the 0-1 Ma portion of the LR04 stack (Lisiecki and Raymo, 2005). Non-normalised OSL and  $\delta^{18}\text{O}$  ages are presented in Table S2.

## References

- Adamiec, G., Aitken, M., 1998. Dose-rate conversion factors: update. *Ancient TL* 16, 37-50.
- Adkins, J., deMenocal, P., Eshel, G., 2006. The "African humid period" and the record of marine upwelling from excess  $^{230}\text{Th}$  in Ocean Drilling Program Hole 658C. *Paleoceanography* 21.
- Aitken, M.J., 1985. Thermoluminescence dating. Academic press.
- Anderson, R.F., LeHuray, A.P., Fleisher, M.Q., Murray, J.W., 1989. Uranium deposition in saanich inlet sediments, vancouver island. *Geochimica et Cosmochimica Acta* 53, 2205-2213.
- Armitage, S.J., 2015. Optically stimulated luminescence dating of Ocean Drilling Program core 658B: Complications arising from authigenic uranium uptake and lateral sediment movement. *Quat Geochronol* 30, 270-274.
- Armitage, S.J., Bailey, R.M., 2005. The measured dependence of laboratory beta dose rates on sample grain size. *Radiat Meas* 39, 123-127.
- Armitage, S.J., Bristow, C.S., Drake, N.A., 2015. West African monsoon dynamics inferred from abrupt fluctuations of Lake Mega-Chad. *P Natl Acad Sci USA* 112, 8543-8548.
- Armitage, S.J., King, G.E., 2013. Optically stimulated luminescence dating of hearths from the Fazzan Basin, Libya: A tool for determining the timing and pattern of Holocene occupation of the Sahara. *Quat Geochronol* 15, 88-97.
- Berger, G.W., 2006. Trans-arctic-ocean tests of fine-silt luminescence sediment dating provide a basis for an additional geochronometer for this region. *Quaternary Science Reviews* 25, 2529-2551.
- Berger, G.W., 2009. Zeroing tests of luminescence sediment dating in the Arctic Ocean: Review and new results from Alaska-margin core tops and central-ocean dirty sea ice. *Global and Planetary Change* 68, 48-57.
- Berger, G.W., 2011. Surmounting luminescence age overestimation in Alaska-margin Arctic Ocean sediments by use of 'micro-hole' quartz dating. *Quaternary Science Reviews* 30, 1750-1769.
- Collins, L.G., Hounslow, M.W., Allen, C.S., Hodgson, D.A., Pike, J., Karloukovski, V.V., 2012. Palaeomagnetic and biostratigraphic dating of marine sediments from the Scotia Sea, Antarctica: First identification of the Laschamp excursion in the Southern Ocean. *Quat Geochronol* 7, 67-75.
- Cunningham, A.C., Wallinga, J., 2010. Selection of integration time intervals for quartz OSL decay curves. *Quat Geochronol* 5, 657-666.
- deMenocal, P., Ortiz, J., Guilderson, T., Adkins, J., Sarnthein, M., Baker, L., Yarusinsky, M., 2000. Abrupt onset and termination of the African Humid Period: Rapid climate responses to gradual insolation forcing. *Quaternary Science Reviews* 19, 347-361.
- Duller, G., 2007. Assessing the error on equivalent dose estimates derived from single aliquot regenerative dose measurements. *Ancient TL* 25, 15-24.
- Duller, G.A.T., 2003. Distinguishing quartz and feldspar in single grain luminescence measurements. *Radiat Meas* 37, 161-165.
- Durcan, J.A., 2012. Luminescence dating of sediments in Punjab, Pakistan: Implications for the collapse of the Harappan Civilisation. Aberystwyth University.
- Durcan, J.A., King, G.E., Duller, G.A.T., 2015. DRAC: Dose Rate and Age Calculator for trapped charge dating. *Quat Geochronol* 28, 54-61.
- Faugères, J.C., Mulder, T., 2011. Contour currents and contourite drifts, *Developments in Sedimentology*, pp. 149-214.
- Galbraith, R.F., Roberts, R.G., Laslett, G.M., Yoshida, H., Olley, J.M., 1999. Optical dating of single and multiple grains of quartz from Jinmium rock shelter, northern Australia: Part I, experimental design and statistical models. *Archaeometry* 41, 339-364.
- Guérin, G., Mercier, N., Adamiec, G., 2011. Dose-rate conversion factors: Update. *Ancient TL* 29, 5-8.
- Henderson, G.M., Anderson, R.F., 2003. The U-series toolbox for palaeoceanography, in: Bourdon, B., Henderson, G.M., Lundstrom, C.C., Turner, S.P. (Eds.), *Uranium-series geochemistry*. Geochemical Society and Mineralogical Society of America, Washington, p. 656.

- Jain, M., Choi, J.H., Thomas, P.J., 2008. The ultrafast OSL component in quartz: Origins and implications. *Radiat Meas* 43, 709-714.
- Jakobsson, M., Backman, J., Murray, A., Løvlie, R., 2003. Optically stimulated luminescence dating supports central arctic ocean cm-scale sedimentation rates. *Geochemistry, Geophysics, Geosystems* 4.
- Lisiecki, L.E., Raymo, M.E., 2005. A Pliocene-Pleistocene stack of 57 globally distributed benthic  $\delta$  18O records. *Paleoceanography* 20, 1-17.
- Lowick, S.E., Preusser, F., 2011. Investigating age underestimation in the high dose region of optically stimulated luminescence using fine grain quartz. *Quat Geochronol* 6, 33-41.
- Matthews, I.P., Trincardi, F., Lowe, J.J., Bourne, A.J., MacLeod, A., Abbott, P.M., Andersen, N., Asioli, A., Blockley, S.P.E., Lane, C.S., Oh, Y.A., Satow, C.S., Staff, R.A., Wulf, S., 2015. Developing a robust tephrochronological framework for Late Quaternary marine records in the Southern Adriatic Sea: New data from core station SA03-11. *Quaternary Science Reviews* 118, 84-104.
- McGee, D., deMenocal, P.B., Winckler, G., Stuut, J.B.W., Bradtmiller, L.I., 2013. The magnitude, timing and abruptness of changes in North African dust deposition over the last 20,000 yr. *Earth Planet Sc Lett* 371-372, 163-176.
- Murray, A., Buylaert, J.P., Henriksen, M., Svendsen, J.I., Mangerud, J., 2008. Testing the reliability of quartz OSL ages beyond the Eemian. *Radiat Meas* 43, 776-780.
- Murray, A.S., Funder, S., 2003. Optically stimulated luminescence dating of a Danish Eemian coastal marine deposit: A test of accuracy. *Quaternary Science Reviews* 22, 1177-1183.
- Murray, A.S., Svendsen, J.I., Mangerud, J., Astakhov, V.I., 2007. Testing the accuracy of quartz OSL dating using a known-age Eemian site on the river Sula, northern Russia. *Quat Geochronol* 2, 102-109.
- Murray, A.S., Wintle, A.G., 2000. Luminescence dating of quartz using an improved single-aliquot regenerative-dose protocol. *Radiat Meas* 32, 57-73.
- Olley, J.M., Pietsch, T., Roberts, R.G., 2004. Optical dating of Holocene sediments from a variety of geomorphic settings using single grains of quartz. *Geomorphology* 60, 337-358.
- Richards, M.A., 1994. Luminescence dating of quartzite from the Diring Yuriakh site., MA Thesis, Simon Fraser University.
- Roberts, R.G., Galbraith, R.F., Olley, J.M., Yoshida, H., Laslett, G.M., 1999. Optical dating of single and multiple grains of quartz from Jinmium rock shelter, northern Australia: Part II, results and implications. *Archaeometry* 41, 365-395.
- Ruddiman, W., Sarnthein, M., Baldauf, J., al., e., 1988. Proceedings of the Ocean Drilling Program Part A - Initial Reports.
- Skonieczny, C., Paillou, P., Bory, A., Bayon, G., Biscara, L., Crosta, X., Eynaud, F., Malaizé, B., Revel, M., Aleman, N., Barusseau, J.P., Vernet, R., Lopez, S., Grousset, F., 2015. African humid periods triggered the reactivation of a large river system in Western Sahara. *Nature Communications* 6.
- Stokes, S., Ingram, S., Aitken, M.J., Sirocko, F., Anderson, R., Leuschner, D., 2003. Alternative chronologies for Late Quaternary (Last Interglacial-Holocene) deep sea sediments via optical dating of silt-sized quartz. *Quaternary Science Reviews* 22, 925-941.
- Wallinga, J., Murray, A., Duller, G., 2000. Underestimation of equivalent dose in single-aliquot optical dating of feldspars caused by preheating. *Radiat Meas* 32, 691-695.
- Wintle, A.G., Huntley, D.J., 1979. Thermoluminescence dating of a deep-sea sediment core. *Nature* 279, 710-712.
- Wintle, A.G., Murray, A.S., 2006. A review of quartz optically stimulated luminescence characteristics and their relevance in single-aliquot regeneration dating protocols. *Radiat Meas* 41, 369-391.